




Cite this: *Chem. Commun.*, 2023, 59, 2481

Received 3rd October 2022,
Accepted 31st January 2023

DOI: 10.1039/d2cc05408f

rsc.li/chemcomm

A NIR fluorescent probe for the detection of renal damage based on overrepresentation of alanine aminopeptidase enzyme†

Marcia Domínguez,^{ab} Kathleen Meyer,^c Félix Sancenón,^{abde} Juan F. Blandez,^{*abd} Manuel Serrano^{*cf} and Ramón Martínez-Máñez ^{*abde}

Kidney damage generates changes at the phenotypic and genotypic levels that allow its monitoring using different biomarkers in blood, urine or serum. Among these biomarkers, kidney failure causes the urine overrepresentation of the alanine aminopeptidase (APN) enzyme. Here, we describe the design of a molecular probe (NB-ALA) based on the Nile Blue fluorophore (NB), which can detect the APN enzyme in urine by simple fluorometric measurements.

The kidneys' primary function is to filter waste products from the blood and remove excess water. In addition, the kidneys are responsible for preserving the balance of salts and minerals (such as calcium, phosphorus, sodium, and potassium), controlling blood pressure, regulating the production of erythropoietin to prevent anemia, and maintaining the body homeostasis. However, the kidneys are very sensitive organs that can suffer from a large number of pathologies that lead to renal fibrosis in the majority of cases. Early-stage detection of these diseases is of great importance because they usually progress over time, increasing the damage and difficulty of recovery treatments.^{1,2}

One of the most common clinical complications in hospitalized and critically ill patients is acute kidney injury.³ There are numerous factors that may predispose to the development of this disease, such as advanced age, chronic infections, diabetes, hypertension, immune disorders, underlying renal and hepatic problems, prostatic hypertrophy and bladder obstruction.⁴

Acute kidney injury is usually diagnosed by the accumulation of end products of nitrogen metabolism (urea and creatinine) or by decreased urine output, or by both factors.⁵ However, serum creatinine cannot be used as a sensitive early biomarker, since it requires a decrease in the glomerular filtration rate of at least 50% and there is a moderately long time lag between this reduction and its translation into an increase in serum levels.^{6,7} Moreover, these levels depend on multiple variables such as age, gender, diet, muscle metabolism, medication, or hydration. In the same way, serum urea levels may increase under certain conditions such as corticosteroid treatment, gastrointestinal bleeding, or a high-protein diet, limiting its use as a renal dysfunction biomarker.^{8,9} Besides changes in creatinine or urea serum levels, kidney damage also induces urinary overrepresentation of the enzyme alanine aminopeptidase (APN). Aminopeptidases degrade the N-terminal residue of oligopeptides, producing smaller peptides and free amino acids. APN is an exopeptidase located in the renal microvillus membranes of the brush border/proximal renal epithelial cells and other plasmatic membranes within the intestines. Upon damage of the renal epithelium, enzymes such as APN are released and secreted into the urine.^{10–12} As a result, their presence in urine can be employed as a kidney degradation biomarker even when urinary macroglobulin remains in normal ranges, allowing their use as an early biomarker of renal damage.^{13,14} APN has also been used as a cancer biomarker and several fluorogenic molecular probes had been developed for its monitoring.^{15,16} However, APN detection in urine samples as a potential early biomarker of kidney damage is a much less explored field (Table S1, ESI†).^{10,11}

Based on the above and following our interest in designing fluorogenic probes for the detection of biomarkers,^{17,18} we

^a Instituto Interuniversitario de Investigación de Reconocimiento Molecular y Desarrollo Tecnológico (IDM), Universitat Politècnica de València, Universitat de València, Spain

^b CIBER de Bioingeniería, Biomateriales y Nanomedicina, Instituto de Salud Carlos III, Spain

^c Institute for Research in Biomedicine (IRB Barcelona), Barcelona Institute of Science and Technology (BIST), Barcelona, 08028, Spain.
E-mail: manuel.serrano@irbbarcelona.org

^d Unidad Mixta de Investigación en Nanomedicina y Sensores, Universitat Politècnica de València, Instituto de Investigación Sanitaria La Fe, Spain.
E-mail: juablaba@upvnet.upv.es, rmaez@qim.upv.es

^e Unidad Mixta UPV-CIPF de Investigación en Mecanismos de Enfermedades y Nanomedicina, Universitat Politècnica de València, Centro de Investigación Príncipe Felipe, Spain

^f Catalan Institution for Research and Advanced Studies (ICREA), Barcelona, 08010, Spain

† Electronic supplementary information (ESI) available. See DOI: <https://doi.org/10.1039/d2cc05408f>



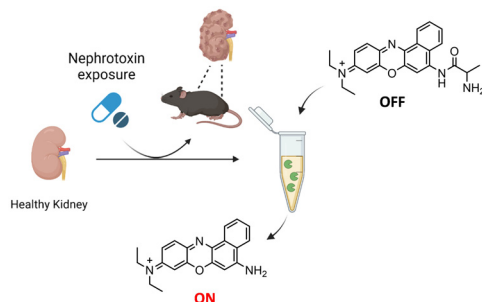


Fig. 1 Schematic representation of the application of the **NB-ALA** probe for the detection of kidney damage through urine samples.

report herein the design and preparation of compound **NB-ALA**, which is a fluorescent APN probe based on Nile Blue (**NB**). **NB** is a low-cost commercial fluorophore that meets the requirements established by the Food and Drug Administration (FDA) for use in humans and whose emission band is centered in the near-infrared area (NIR).¹⁹ **NB-ALA** can sensitively and selectively detect the enzyme APN in aqueous solutions and in doped urine. Besides, APN detection by **NB-ALA** is also validated in a murine model of acute kidney injury by direct urine fluorescence measurements (Fig. 1).

NB-ALA was synthesized using a two-step protocol (Fig. S1, ESI†). In the first step, Fmoc-Ala-OH was covalently linked through the formation of an amide bond with the **NB** fluorophore. Then, in the second step, the Fmoc protecting group was removed with piperidine, yielding **NB-ALA** with a 31% global yield. **NB-ALA** and its intermediate were characterized by ¹H-NMR, ¹³C-NMR and mass spectrometry (see ESI†). **NB-ALA** was designed in such a way that, after APN hydrolysis, **NB** was released (Fig. 2A). H₂O–DMSO 99:1 v/v solution of **NB-ALA** shows a weak emission band at 630 nm upon excitation at 530 nm ($\Phi_{\text{NB-ALA}} = 0.00028$). However, in the presence of APN enzyme, a *ca.* 10-fold enhancement in emission band at 630 nm was observed (Fig. 2B, $\Phi_{\text{NB}} = 0.01$ and Table S2, ESI†). This emission enhancement is ascribed to the APN-induced hydrolysis of the **NB-ALA** probe, which yields free **NB** (Fig. 2A).

HPLC-MS studies, carried out with **NB-ALA** probe alone and in the presence of APN enzyme, confirmed the proposed hydrolysis reaction. In this respect, the chromatogram of the probe alone showed a single peak at 6.02 min whereas after 15 min in the presence of enzyme the intensity of this signal is reduced with the subsequent appearance of a new peak at 5.47 min, which is ascribed to **NB** formed upon **NB-ALA** hydrolysis (Fig. 2C and Fig. S4, ESI†). Besides, after 30 min of enzyme addition the 6.02 min peak of **NB-ALA** completely disappeared confirming the complete hydrolysis of the probe.

In an additional study, different amounts of APN were added to a solution of **NB-ALA** (H₂O–DMSO 99:1 v/v, 20 μM) and the emission spectra ($\lambda_{\text{exc}} = 530 \text{ nm}$) were recorded after incubation of the samples at 37 °C for 30 min. The activity of the APN enzyme was calculated as 22.1 mU mL^{-1} , using Ala-7-amido-4-methylcoumarin (Ala-AMC) as a reference substrate (Fig. S5 and eqn (S1), ESI†). As shown in Fig. 3A, a marked emission

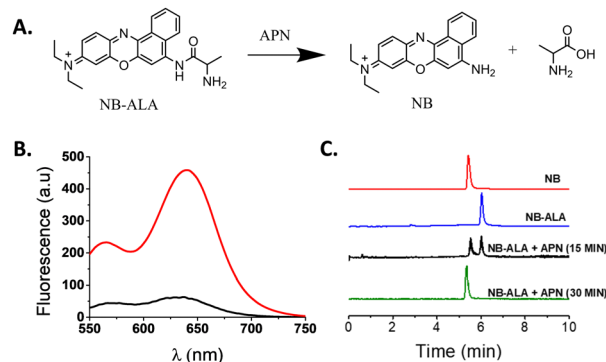


Fig. 2 (A) APN-induced hydrolysis of the **NB-ALA** probe. (B) Fluorescence emission of **NB-ALA** (20 μM) + APN (2 $\mu\text{g mL}^{-1}$, 22.1 mU mL^{-1}) (red curve) and **NB-ALA** (20 μM) (black curve) in water/DMSO 99:1 v/v at pH 7.4 ($\lambda_{\text{exc}} = 530 \text{ nm}$), after 30 minutes upon APN enzyme addition. (C) Chromatograms of aqueous free **NB-ALA** (20 μM) (blue), free **NB** (20 μM) (red), and **NB-ALA** (20 μM) + APN (2 $\mu\text{g mL}^{-1}$, 22.1 mU mL^{-1}) after 15 minutes (black) and after 30 min (green) of enzyme addition. Conditions: KromasilC18 column, 0.7 mL min^{-1} , acetonitrile–MeOH gradient elution from 70:30 v/v at 0 min to 50:50 v/v at 15 min.

enhancement was observed proportional to the amount of enzyme added and due to the APN enzyme induced hydrolysis of **NB-ALA** and the subsequent release of free **NB**. From these data, a limit of detection for APN as low as 1 ng mL^{-1} was calculated using the eqn (S2) (Fig. S6, ESI†).

Additionally, a kinetic study of **NB-ALA** hydrolysis in the presence or absence of the APN enzyme (2 $\mu\text{g mL}^{-1}$, 22.1 mU mL^{-1}) was carried out (Fig. 3B). The fluorescence emission of the **NB-ALA** solution (H₂O–DMSO 99:1 v/v, 20 μM) remained stable in the absence of APN enzyme. In sharp contrast, upon the addition of the APN enzyme (2 $\mu\text{g mL}^{-1}$, 22.1 mU mL^{-1}), a progressive fluorescence enhancement at

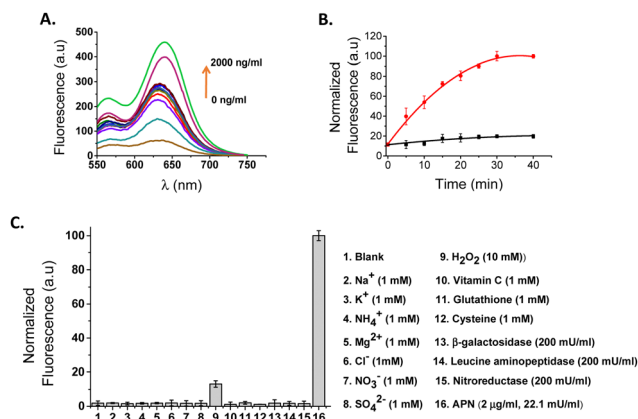


Fig. 3 (A) Fluorescence emission spectra of **NB-ALA** (20 μM) in aqueous solution (H₂O–DMSO 99:1 v/v, pH 7.4) in the presence of different concentrations of APN enzyme (0–2000 ng mL^{-1}). (B) Fluorescence of **NB-ALA** in (H₂O–DMSO 99:1 v/v, pH 7.4) at different time points in the absence (black curve) and in the presence of APN enzyme (2 $\mu\text{g mL}^{-1}$) with an activity of 22.1 mU mL^{-1} (red curve). Error bars are expressed as 3 σ for three independent experiments. (C) Selectivity of **NB-ALA**. (H₂O–DMSO 99:1 v/v, pH 7.4). **NB-ALA** (20 μM) was incubated with the following interferents.



630 nm due to **NB** was observed reaching the maximum in *ca.* 30 min (Table S3, ESI†). Finally, the emission response of **NB-ALA** in the presence of potentially interfering species such as anions, cations, small biomolecules (vitamin C, glutathione, cysteine) and enzymes (β -galactosidase, leucine aminopeptidase, nitroreductase, APN) was also tested (Fig. 3C). This study demonstrated that only in the presence of APN was a marked emission enhancement at 630 nm observed.

Considering the promising results obtained with **NB-ALA** in aqueous solutions, we checked the ability of the probe to detect APN in a more clinically relevant environment. For this purpose, a human urine sample was collected from a healthy volunteer. The concentration of APN enzyme was negligible in this urine as confirmed using the aminopeptidase N/ANPEP ELISA kit (see ESI†, Table S4). In order to validate the ability of the probe for APN enzyme detection in urine, **NB-ALA** was added to human urine samples that were doped with different amounts of APN (probe concentration 20 μ M). The fluorescence signal was recorded after incubation at 37 °C for 30 min (Fig. 4A). A progressive emission enhancement was obtained directly related to the amount of APN (5-fold at 2 μ g mL⁻¹ of enzyme, 22.1 mU mL⁻¹). From the obtained calibration curve (Fig. 4B) a limit of detection of 5.4 ng mL⁻¹ for APN in doped human urine was calculated using eqn (S2) (see ESI†).

Subsequently, the urine sample was spiked with different amounts of APN (50, 100 and 200 ng mL⁻¹), **NB-ALA** was added, and the mixture was incubated at 37 °C for 30 min. Finally, the emission at 630 nm was measured and the APN concentration was calculated using the calibration curve shown in Fig. 4B. The obtained results are shown in Table 1. The probe **NB-ALA** successfully detected APN in human urine spiked with the enzyme with recoveries ranging from 98.5 to 99.0%.

To test the ability of **NB-ALA** to detect endogenous APN enzyme in a pre-clinical setting, urine samples from mice with acute kidney damage and fibrosis were evaluated. To generate acute kidney damage, C57BL/6 J mice were one time injected intraperitoneally (i.p.) with a high concentration (250 mg kg⁻¹) of folic acid (FA), which is a well-known experimental model of kidney damage.²⁰ The pathological features underlying FA-induced acute kidney injury are direct and indirect tubular damage and oxidative stress, which triggers tubular epithelial cell (TEC) necrosis, senescence, and cytokine release.²¹ In this

Table 1 Determination of APN in human urine

APN spiked (ng mL ⁻¹)	APN detected (ng mL ⁻¹)	% of APN found by NB-ALA
50	49.5	99.0
100	98.5	98.5
200	197.8	98.9

model, serum urea and serum creatinine levels recover with time (or rather compensates while some renal damage remains) (Fig. 5D)²² and the only pathological reading that can be related to renal damage is urine density, which was monitored with time.

Urine samples of FA-treated mice were collected at 0 (control, CTR), 7 and 15 days after FA injection (Fig. 5A). To analyse the animal model, the mice were euthanized, the kidneys were harvested, and tissue sections were embedded in paraffin and stained with Sirius red/Fast green in order to visualize and quantify fibrosis (Fig. 5B, C and Fig. S7, ESI†). CTR animals did

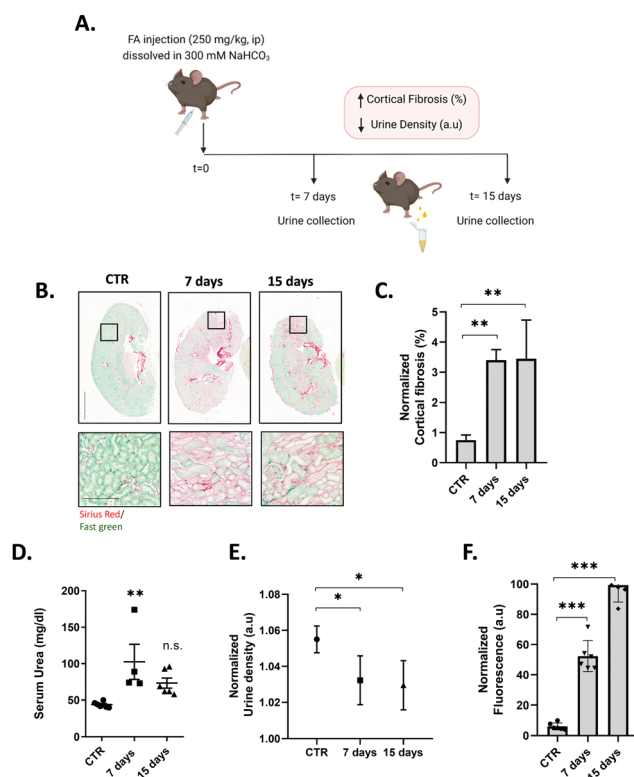


Fig. 5 **NB-ALA** detection in urine of mice exposed to FA-induced kidney injury. (A) Timeline for the experimental procedure of FA-induced kidney injury. 8–10-week-old male BL6/J mice were treated intraperitoneally with 250 mg kg⁻¹ folic acid dissolved in 300 mM sodium bicarbonate buffer. After 0, 7 and 15 days, urine was collected ("spot" urine) and the mice were sacrificed. (B) Kidneys were harvested, paraffin-embedded, sectioned and stained for Sirius red/Fast green (fibrosis). Bar graphs within the upper row (whole kidneys) represent 250 mm and in the lower row (magnification) 250 μ m. (C) Quantification of renal fibrosis. $n = 6$; ** $P = 0.0011$. (D) Quantification of serum urea. For 7 days, $n = 4$; ** $P = 0.0066$ and for 15 days, $n = 6$, n.s. $P = 0.1183$. (E) Urine density measured with a refractometer. $n = 6$; * $P = 0.0113$. (F) Fluorescence emission intensity of **NB-ALA** in urine samples. $n = 6$; *** $P < 0.001$.

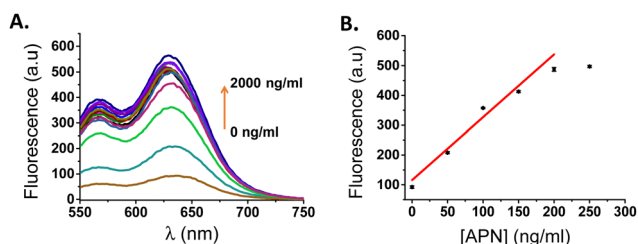


Fig. 4 (A) Fluorescence emission spectra of **NB-ALA** in human urine samples (20 μ M) doped with different concentrations of APN (0–2000 ng mL⁻¹, 22.1 mU mL⁻¹) after 30 min. (B) Calibration curve for the APN concentration in urine. Error bars are expressed as 3 σ for three independent experiments.



not present signs of cortical fibrosis, whereas mice after 7 and 15 days of FA treatment developed fibrosis. In order to assess whether fibrosis resulted in a decline of renal function, urine was collected, and their density measured (Fig. 5E), showing a significative reduction in the values for sample of animals after 7 and 15 days of FA treatment, corroborating renal failure.

To validate the effectiveness of **NB-ALA** in determining kidney failure by APN detection, urine samples collected at 0, 7 and 15 days were treated with **NB-ALA** (final concentration of 20 μM) and incubated at 37 $^{\circ}\text{C}$ for 30 min before measuring the fluorescence emission signal at 630 nm ($\lambda_{\text{exc}} = 530 \text{ nm}$). Fluorescence measurements were performed without any previous treatment of urine (Fig. 5F). Interestingly, significant differences in fluorescence signal were found in urine samples 7 days after FA treatment (6-fold). Furthermore, urine samples from 15 days FA post-treatment showed an 11-fold enhancement. These experiments demonstrate that the **NB-ALA** can be used for the detection of renal damage in a mouse model of kidney injury.

In summary, we show herein the synthesis and characterization of **NB-ALA**, a NIR fluorescent probe for APN detection. **NB-ALA** is weakly emissive, however, in the presence of APN enzyme, **NB-ALA** is hydrolysed releasing the highly emissive **NB** fluorophore. **NB-ALA** was functional in water and in APN-doped human urine samples. Additionally, the **NB-ALA** probe was validated in a murine renal fibrosis model induced by FA. An emission signal was only observed in urine from fibrotic kidneys of FA-treated mice. This study demonstrates the potential applications of the **NB-ALA** probe for the sensitive and selective detection of APN to non-invasively determine the burden of renal damage. **NB-ALA** is a promising probe that could be employed for a range of applications including the monitoring of treatments with nephrotoxic drugs that induce acute kidney damage or to determine regeneration after renal damage.

The authors thank the Spanish Government (PID2021-126304OB-C41) and the Generalitat Valenciana (PROMETEO CIPROM/2021/007) for support and acknowledge the financial support from the FEDER fund of the European Union (IDIFEDER/2021/044). This work was also supported by CIBER-Consorcio Centro de Investigación Biomédica en Red-(CB06/01/2012), Instituto de Salud Carlos III, Ministerio de Ciencia e Innovación. M. D.-R. is grateful for his predoctoral fellowship

Grisolias to the Generalitat Valenciana (GRISOLIAP/2019/144). J. F. B. is thankful for his postdoctoral fellowship Sara Borrell from ISCIII (CD19/00038).

Conflicts of interest

There are no conflicts to declare.

Notes and references

- 1 J. G. Abuelo, *N. Engl. J. Med.*, 2007, **357**, 797–805.
- 2 L. He, Q. Wei and J. Liu, *et al.*, *Kidney Int.*, 2017, **92**(5), 1071–1083.
- 3 J. A. Kellum, P. Romagnani, G. Ashuntantang, C. Ronco, A. Zarbock and H.-J. Anders, *Nat. Rev. Dis. Primers*, 2021, **7**, 52.
- 4 S. M. Bagshaw and R. Bellomo, *Curr. Opin. Crit. Care*, 2007, **13**(6), 638–644.
- 5 J. Y. C. Soo, J. Jansen, R. Masereeuw and M. H. Little, *Nat. Rev. Nephrol.*, 2018, **14**, 378–393.
- 6 X. Wang, *et al.*, *J. Am. Soc. Nephrol.*, 2006, **17**, 2900–2909.
- 7 P. K. Bhatraju, *et al.*, *JAMA Netw. Open*, 2020, **3**, 1–12.
- 8 M. A. Perazella and S. G. Coca, *Nat. Rev. Nephrol.*, 2013, **9**, 484–490.
- 9 O. Dong-Jin, *Renal Failure*, 2020, **42**(1), 154–165.
- 10 P. Cheng, Q. Miao, J. Huang, J. Li and K. Pu, *Anal. Chem.*, 2020, **92**, 6166–6172.
- 11 X. He, Y. Xu, W. Shi and H. Ma, *Anal. Chem.*, 2017, **89**(5), 3217–3221.
- 12 L. Z. Chen, W. Sun, W. H. Li, J. Li, L. P. Du, W. F. Xu, H. Fang and M. Y. Li, *Anal. Methods*, 2012, **4**, 2661–2663.
- 13 L. Z. Chen, W. Sun, J. Li, Z. Z. Liu, Z. Ma, W. Zhang, L. P. Du, W. F. Xu, H. Fang and M. Y. Li, *Org. Biomol. Chem.*, 2013, **11**, 378–382.
- 14 J. Li, L. Z. Chen, W. X. Wu, W. Zhang, Z. Ma, Y. N. Cheng, L. P. Du and M. Y. Li, *Anal. Chem.*, 2014, **86**, 2747–2751.
- 15 H. Li, Q. Yao, W. Sun, K. Shao, Y. Lu, J. Chung, D. Kim, J. Fan, S. Long, J. Du, Y. Li, J. Wang, J. Yoon and X. Peng, *J. Am. Chem. Soc.*, 2020, **142**(13), 6381–6389.
- 16 X. Zhou, H. Li, Ch Shi, F. Xu, Z. Zhang, Q. Yao, H. Ma, W. Sun, K. Shao, J. Du, S. Long, J. Fan, J. Wang and X. Peng, *Biomaterials*, 2020, **253**, 120089.
- 17 M. Xiao, W. Sun, J. Fan, J. Cao, Y. Li, K. Shao, M. Li, X. Li, Y. Kang, W. Zhang, S. Long, J. Du and X. Peng, *Adv. Funct. Mater.*, 2018, **1805128**, 1–9.
- 18 W. Sun, S. Guo, C. Hu, J. Fan and X. Peng, *Chem. Rev.*, 2016, **116**, 7768–7817.
- 19 J. Mérian, J. Gravier, F. Navarro and I. Texier, *Molecules*, 2012, **17**, 5564–5591.
- 20 Z. Hu, H. Zhang, S. Yang, X. Wu, D. He, K. Cao and W. Zhang, *Oxid. Med. Cell. Longevity*, 2019, **8**, 1–9.
- 21 O. E. Aparicio-Trejo, P. Rojas-Morales, S. H. Avila-Rojas, J. C. León-Contreras, R. Hernández-Pando, A. P. Jiménez-Urbe, R. Prieto-Carrasco, L. G. Sánchez-Lozada, J. Pedraza-Chaverri and E. Tapia, *Int. J. Mol. Sci.*, 2020, **21**, 6512.
- 22 J. A. Kellum, *Crit. Care Clin.*, 2015, **31**, 621–632.

